euronoise

Active control of multimodal tonal noise propagated in circular duct with axial subsonic mean flow until M=0.3

Martin Glesser[a], Emmanuel Friot[b], Muriel Winninger[a], Cédric Pinhède[a] and Alain Roure[a]

[a]CNRS - LMA, 31 Chemin Joseph Aiguier, 13009 Marseille, France
[b]Laboratory for Mechanics and Acoustics CNRS, 31 chemin Joseph Aiguier, 13009 Marseille, France
glesser@lma.cnrs-mrs.fr

Since a new generation of aircraft engines with lower blade passing frequencies was developed in the 90's, the fan tone radiated from the inlets has become one of the main sources of sound. Efforts have then been made to develop active noise control. Although encouraging results have been obtained, the physical limitations involved in tone reduction have not been clearly determined, owing mainly to the complexity of the experimental rigs used. An experimental study is presented here on the control of multimodal tonal noise propagating in circular ducts in the presence of a mean flow with Mach number $M \leq 0.3$. A laboratory wind tunnel was used for this purpose. Two factors limiting the sound reduction are thus observed: (i) the degradation of the secondary transfer matrix conditioning as the number of propagating modes increases in the duct and (ii) the degradation of the system time-invariance hypothesis as the flow velocity increases. The effects of these limiting factors on the efficiency of the noise control are assessed.

1 Introduction

Since the 90's, efforts have been made to develop active noise control to reduce aircraft fan tone radiation which is one of the main source of sound, especially during landing [1]. Although passive absorbers efficiently reduce the high frequency components, they do not suffice to reduce the relatively low frequency tonal noises involved [2]. Many efforts have then been made to develop active noise control methods. Analytical models of control [3, 4] and experiments performed under no-flow conditions [5, 6] have shown the potential of active techniques to reduce the radiated tones. Experiments have also been carried out on reduced scale turbines [7, 8]. Encouraging results have been obtained but the physical factors limitating fan tone reduction have not been clearly determined, mainly due to the complexity of the experimental rigs used (the high operating cost, the often impossible instrumentation and the difficult to monitor noise generation).

In this context, the French research project CoMBE (Contrôle et Métrologie du Bruit en Ecoulement) was set up to investigate the effects of the mean flow ($M \leq 0.3$, which is close to the flow velocity encountered in aircraft engines during airport approaches) on (i) the propagation of multimodal tonal noise in circular ducts and (ii) the control of these tones. A laboratory wind tunnel was used for this purpose. This tunnel consists of a PVC flow-duct (with axial subsonic mean flow) which is easily instrumentable (with a microphone array and laser doppler anemometer in particular) . High amplitude (up to 135 dB ref. 2.10^{-5} Pa) multimodal tonal noise can be generated by a multichannel primary source. The tone production and the flow generation can be monitered independently.

The aim of this study was to optimize a system designed to control the tones propagating along the wind tunnel and to assess its performances (its efficiency and physical limits). Keeping in mind the practical aim of aircraft engine tonal noise reduction, an adaptive active noise control (ANC) strategy not requiring any in-situ transducer calibration or preliminary modal analysis, was adopted. As a reference signal synthesized from the engine speed is available for practical applications, a feedforward FXLMS (Filtered-Reference Least Mean Square) control strategy was used [9]. The minimization microphones were flush-mounted on the duct walls as, for obvious practical reasons, they cannot be placed in the far field, where the radiated sound field had to be minimized. The aim of the control system was therefore to achieve a global control of the sound field in the duct in order to reduce the sound power radiated, from the nacelle, in the far field [7].

This paper is organized as follows: after describing the experimental set-up, the results of active noise control experiments performed in three configurations are presented and discussed. The first configuration intends to be consistent with the application to aircraft engine noise: with flow at an excitation frequency insuring the propagation of six independent acoustic modes. Two physical limitations of the control system are described in two simplified configurations: with flow at an excitation frequency insuring the propagation of the planar acoustic mode only and without flow at different excitation frequencies.

2 Material and methods

2.1 Experimental set-up

The experimental set-up used here was composed of a blower creating an air jet passing through a flow stabilization section and an instrumented duct (see Figure 1). The duct is built-up with 10 mm-thick PVC tubes with a diameter of 176 mm. Three main sections can be identified: (i) the primary source section generating the tonal noise to be controlled, (ii) the control section and (iii) the detection section consisting of a microphone array measuring the downstream effects of the control system. GRAS 40PR microphones were used in this study. The flow velocity u, which was measured in the center of the duct section, can be set from 0 to 115 m/s (which corresponds to Mach number ranging between 0 and 0.3). The air flow left the duct under free jet conditions.

The first duct mode cut-off frequencies under no-flow conditions are summarized in Table 1. The noise control experiments were performed up to an excitation frequency of 2450 Hz. At this frequency, six independent acoustic modes can propagate in the duct (the planar mode, the first rotative and counter-rotative azimuthal modes, the second rotative and counter-rotative azimuthal modes and the first radial mode).

2.2 Primary source section

The primary source generating the tonal noise to be controlled consists of a series of eight elementary sources placed axially on the wall of the duct. Each elementary

mode	type of mode	cut-off frequency
p_{00}	planar mode	
p_{10}	azimuthal mode	$f_{10} = 1144$ Hz
p_{20}	azimuthal mode	$f_{20} = 1898$ Hz
p_{01}	radial mode	$f_{01} = 2381$ Hz
p_{30}	azimuthal mode	$f_{30} = 2611$ Hz

Table 1: First duct mode cut-off frequencies.

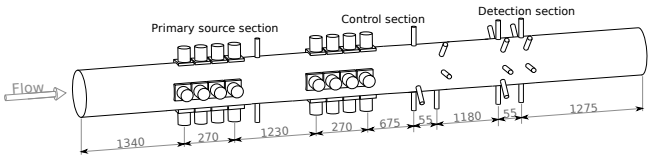

Figure 1: Diagram of the experimental rig (dimensions in mm; scales are not respected).

source consists of two MOREL MDM55 loudspeakers placed face to face, which are excited by the same amplification channel. The successive pairs are placed on perpendicular axes (see Figure 2). The sinusoidal excitation signal $x(t)$ at frequency f_0 (which we have called the excitation frequency) was adapted in terms of the amplitude and phase in order to maximize the sound level reaching a pair of microphones placed downstream. This maximization algorithm which was implemented in the LMA controller NOVACS, favoured the planar mode or imposed the generation of higher-order modes when the relative phase between two transducers in a pair was reversed. In the present case, the six upstream pairs were in phase and the two downstream ones are in phase opposition.

With this source, it was possible to generate 125-dB tonal noise at 800 Hz and 105-dB tonal noise at 2450 Hz, giving a mean ratio between the tone level and the background noise level of 40 dB and 20 dB, respectively, at $M = 0.3$.

2.3 Control section

The control section consisted of a microphone array measuring the signals **e** to be minimized and a multi-channel

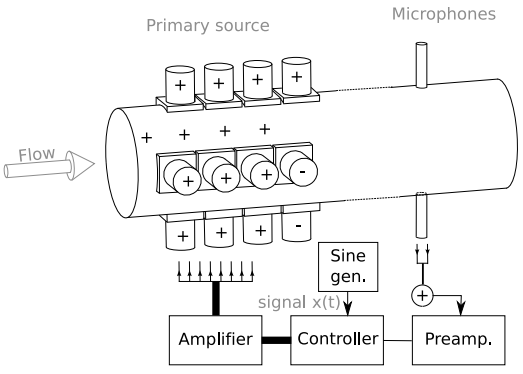

Figure 2: Diagram of the primary source section (scales are not respected). The + and − symbols indicate the relative phase between two transducer in a pair excited by the same amplification channel.

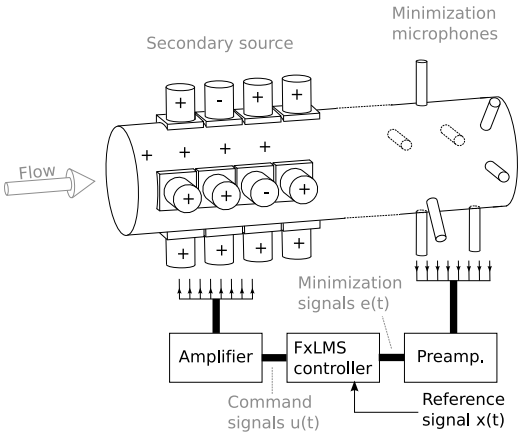

Figure 3: Diagram of the control section (scales are not respected). The + and − symbols indicate the relative phase between two transducers in a pair excited by the same amplification channel.

secondary source (which was identical to the primary source) excited by the command signals **u** calculated by a multi-channel FXLMS controller (see Figure 3).

As stated in the Introduction, a reference signal $x(t)$ describing the primary noise without being affected by the secondary source radiation was used: this was the electric signal feeding the primary sources in the present case. The classical feedforward FXLMS algorithm was then implemented [10, 9]. The corresponding real-time active control algorithm was implemented on the COMPARS multi-processor system at the LMA. In these experiments, the sampling frequency was set to 9 kHz.

If N modes are assumed to be significantly excited in the duct by the primary sources, there will be two conditions (sufficient but not necessary conditions) for the control to be global, (i) the secondary sources must be able to excite the N modes independently and (ii) the minimization microphones must be able to detect the N modes. Since the primary and secondary source networks were identical, the first condition was fulfilled. However, the minimization microphones had to be carefully positioned. Some constraints based on the acoustic mode pattern had to be fullfilled. In this study, since six independent modes had to be controlled (see Table 1), the minimization array configuration shown in Figure 3 was adopted. The singular value decomposition (SVD) of the secondary transfer matrix was used to test this configuration, since the SVD makes it possible to determine how many independent modes contribute to the energy transfers. This SVD is plotted in Figure 4. At frequencies below 1150 Hz (corresponding to the first azimuthal mode cut-off frequency), the matrix is rank-1, in a first approximation, as only one significant singular value is observed. Only one mode (the planar mode) therefore contributes to the energy transfer. At frequencies in the [1150 Hz - 1900 Hz] range, three significant modes are observed (the planar mode and the first rotative and counter-rotative azimuthal modes, see Table 1). In the [1900 Hz - 2380 Hz] range, five significant modes are observed (the planar mode and the first and second rotative and counter-rotative azimuthal modes). At frequencies above 2380 Hz, a sixth signifi-

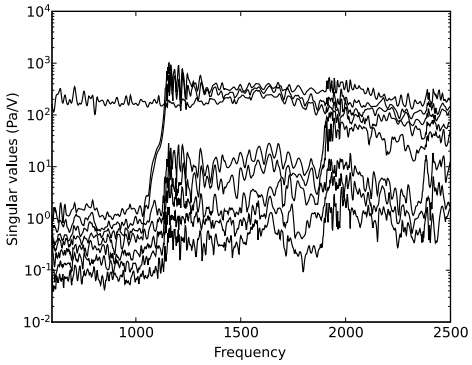

Figure 4: Singular values of the secondary transfer matrix versus the frequency.

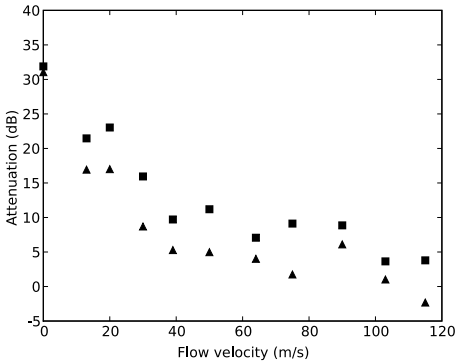

Figure 5: Tonal noise mean attenuation due to the control as a function of the flow velocity, for a 2450 Hz pure tone ■ on the minimization microphones and ▲ on the visualization microphones.

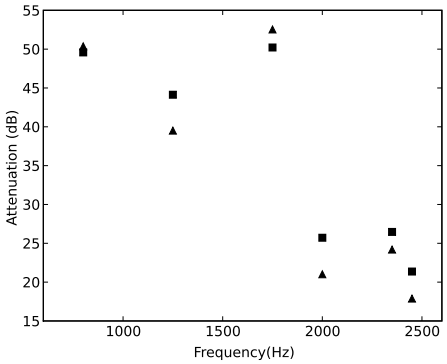

Figure 6: Tonal noise mean attenuation due to the control as a function of the primary source excitation frequency, ■ on the minimization microphones and ▲ on the visualization microphones.

cant mode is less clearly visible (the first radial mode). The increase in the transfer matrix rank observed at each mode cut-off frequency confirms that (i) the secondary sources excite all the modes and that (ii) the minimization microphone-array is able to detect them.

3 Results and discussion

In what follows, the performances of the ANC system are assessed in terms of the tonal noise attenuation resulting from the control process; i.e. the difference between the mean pure tone levels corresponding to the excitation recorded at the minimization or detection microphones, expressed in dB, when the controller is turned on and off.

3.1 In-flow, multimodal

The ANC results obtained at a primary source excitation frequency of 2450 Hz and for a flow velocity ranging between 0 and 115 m/s are presented in Fig. 5. At this frequency, six independent acoustic modes were propagated. The attenuation decreased as the flow velocity increased, until becoming quasi-null at a flow velocity of 115 m/s. The noise control was no longer global, as the attenuation recorded was 5 dB higher on average at the minimization microphones than at the detection microphones.

The control of a 2450 Hz tonal noise were therefore inefficient at $M = 0.3$. The limiting factors will be identified in the next sections by studying two simplified configurations.

3.2 No-flow condition

Figure 6 shows the performance of the controller under no-flow conditions at various primary source excitation frequencies. At excitation frequencies below 1900Hz ($f_0 = 800$ Hz, $f_0 = 1250$ Hz, $f_0 = 1750$ Hz), the decrease in the tone amplitude ranged from 40 dB to 50 dB. The noise control was almost global, as a similar level of tone reduction was observed at both the minimization and detection microphones. At these frequencies, the performances of the ANC can be said to be optimum and to be limited only by the numerical accuracy of the controller. However, the performances of the controller decreased at excitation frequencies above 1900 Hz ($f_0 = 2000$ Hz, $f_0 = 2350$ Hz, $f_0 = 2450$ Hz), giving a tone reduction ranging between 15 dB and 25 dB.

At high frequencies, the controller may fail to control some of the propagating modes, which would explain the decrease in the efficiency of the ANC, which depends on the properties of the secondary transfer matrix $\mathbf{H}$. This matrix fails to describe response of the physical system to be controlled if the transducers are badly positioned (i.e. if the minimization microphone array is not able to detect all the modes excited by the primary source or if the secondary sources are not able to control them). The adequate positioning of the transducers (see section 2.3) invalidate this hypopthesis.

A second hypothesis is now proposed: the conditioning of the matrix $\mathbf{H}$ may be responsible for the decrease in the ANC performances. If the spreading of the significant singular values of the secondary transfer matrix is large (i.e. if the ratio between the largest and smallest singular value is large), the matrix is said to be ill-conditioned. This property of the matrix $\mathbf{H}$ affects the performances of the ANC, as poor conditioning results

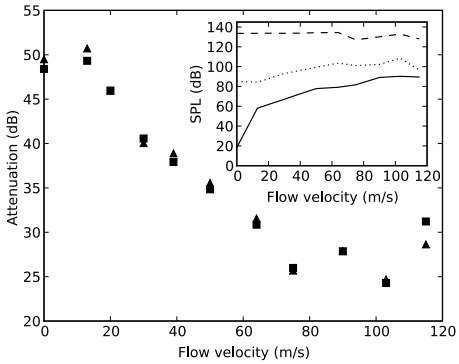

Figure 7: Tonal noise mean attenuation due to the control as a function of the flow velocity, for a 800 Hz pure tone ■ on the minimization microphones and ▲ on the visualization microphones. The inset figure depicts the tonal noise magnitude measured, as a function of the flow velocity *dashed line* without control, *dotted line* with control and *solid line* without primary noise (SPL in dB ref. 2.10^{-5} Pa).

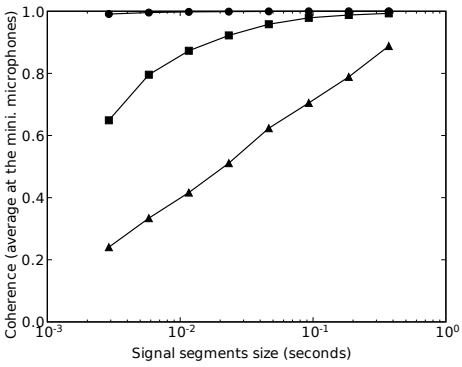

Figure 8: Coherence (average on the minimization microphones) as a function of the signal segments size for: • $u = 19$ m/s, ■ $u = 58$ m/s and ▲ $u = 95$ m/s.

in low convergence of the FXLMS algorithm. The convergence of some individual modes can become slower than the transient time constant of the control system. The poor overall convergence of the FXLMS algorithm will therefore prevent the optimum control performances from being reached [9]. Indeed, the singular values of the secondary transfer matrix shown in Figure 4 shows a considerable spreading at frequencies above the second azimuthal mode cut-off frequency (1898 Hz, see table 1). The conditioning of the matrix $\mathbf{H}$ is therefore responsible for the loss of efficiency of the control system observed at higher excitation frequencies.

3.3 In-flow, planar mode only

The ANC results obtained with a primary source excitation frequency of 800 Hz and a flow velocity ranging between 0 and 115 m/s are presented in Figure 7. At this frequency, only the planar mode propagates in the duct. Between 0 and 15 m/s, the flow velocity does not affect the ANC performances, and an attenuation of about 50 dB is observed, as in the no-flow case. Between flow velocities of 15 and 80 m/s, the attenuation decreases linearly as the flow velocity increases. At higher flow velocities, the attenuation ranges between 25 and 30 dB. The inset in Figure 7 shows the tonal noise magnitude measured with and without the control system along with the background noise at the excitation frequency. It is worth noting that the controlled tonal noise level was always higher then the background noise level. This shows that the ANC performances are not limited by the primary tonal noise emergence, which decreases as the flow velocity increases (due to the increase in the background noise).

Decrease in the ANC performances observed as the flow velocity increased may be attributable to an inaccurate description of the physical system to be controlled. The feedforward ANC system assumes this system to be linear and stationary (or at least slowly non-stationary with respect to the controller's time constants). In the presence of the flow, this hypothesis has to be challenged. The coherence function γ_{ex} between the reference signal $x(t)$ and the signal detected by an error sensor $e(t)$ can be defined by [12]:

$$\gamma_{ex}(\omega_0) = \frac{\left|\left\{\overline{E_m(\omega_0)}X_m(\omega_0)\right\}_m\right|^2}{\left\{|E_m(\omega_0)|^2\right\}_m \cdot \left\{|X_m(\omega_0)|^2\right\}_m}, \quad (1)$$

where $\{.\}_m$ denote time averaging over successive signal segments and $E(\omega_0)$ and $X(\omega_0)$ denote the Fourier transforms of $e(t)$ and $x(t)$, respectively, at the excitation frequency ($f_0 = \omega_0/2\pi$). This function provides information about the linearity of the system. It is plotted as a function of the size of the signal segments used for the time averaging procedure, at the three flow velocities shown in Figure 8.

At $u = 19$ m/s, the coherence was always equal to approximately one, regardless of the size of the time segments used for the calculation. This indicates that the reference signal and the signals given by the error sensors were linearly correlated. In other words, the system to be controlled reacts linearly to the primary source excitation,regardless of the time scale on which it was tested. At $u = 58$ m/s, the coherence was equal to approximately one when calculated taking signal segments of about 0.5 s. When the calculations were based on shorter time segments, the coherence decreased. In comparison with the previous case, it can be concluded that, although the system seems to react linearly to the primary source excitation when observed on a long timescale (more than 10^{-1} s), short-term instabilities make the system non-linear when it is observed on short timescales (below 10^{-1} s). This statement is also true at higher flow velocities ($u = 95$ m/s).

Since this is a real-time adaptive control system, the time-scales used to calculate the command signals are sufficiently short to rule out the possibility that we have been dealing with a linear and stationary physical system. The short-term instabilities due to the flow therefore affect the coherence between the reference and error sensor signals, which reduces the efficiency of the active noise control system: this explains the poor ANC performances observed in Figure 7 at high flow velocities.

4 Conclusion

An active noise control system was optimized for controlling multimodal tonal noise propagated in a flow-duct. An adaptive control strategy based on an FXLMS algorithm, requiring no in-situ transducer calibration or preliminary modal analysis, was adopted. A laboratory wind tunnel was used for this purpose, because it was easily instrumentable and the tone production and flow velocity could be monitored independently. This adaptable set-up lent itself better to studying the efficiency and the physical limitations of the noise control system in question than a reduce-scale turbine installation.

An attenuation of about 20 dB was achieved in the case of a multimodal tonal noise (involving 6 independent modes) without flow. At a flow velocity of $M = 0.3$ f, a monomodal tonal noise was attenuated by about 30 dB. Conversely, the system fails to control a multimodal tonal noise at $M = 0.3$ upwards. Two factors limiting the tone reduction were found to exist: (i) the degradation of the secondary transfer matrix conditioning as the number of propagating modes increases in the duct and (ii) the fact that the hypothesis adopted about the time-invariance of the system to be controlledis not true at higher flow velocities.

These limiting factors need to be addressed independently in further studies, to improve the efficiency of the noise control system and eventually make it applicable in the field of aeronautics.

Acknowledgements

The present study was performed in the framework of the CoMBE project funded by the French "Fondation de Recherche pour l'Aéronautique et l'Espace" (FNRAE) which involves five French laboratories (LEA, LMFA, LAUM, ONERA and LMA). The experiments were performed at the "Laboratoire d'Etudes Aérodynamiques" (LEA) in Poitiers, France.

References

[1] R. H. Thomas, R. A. Burdisso, C. R. Fuller, and W. F. O'Brien. Preliminary experiments on active control of fan noise from a turbofan engine. *Journal of Sound and Vibration*, 161(3):532–537, March 1993.

[2] M. A. Galland, B. Mazeaud, and N. Sellen. Hybrid passive/active absorbers for flow ducts. *Applied Acoustics*, 66(6):691–708, June 2005.

[3] John D. Risi, Ricardo A. Burdisso, and Chris R. Fuller. Analytical investigation of active control of radiated inlet fan noise. *The Journal of the Acoustical Society of America*, 99(1):408–416, 1996.

[4] P. Joseph, P. A. Nelson, and M. J. Fisher. Active control of fan tones radiated from turbofan engines. i. external error sensors. *The Journal of the Acoustical Society of America*, 106(2):766–778, 1999.

[5] P. Joseph, P. A. Nelson, and M. J. Fisher. Active control of fan tones radiated from turbofan engines. ii. in-duct error sensors. *The Journal of the Acoustical Society of America*, 106(2):779–786, 1999.

[6] M. J. Wilkinson and R. F. Joseph. Active control of buzz-saw tones: Experimental results from a laboratory-scale, no-flow rig. *The Journal of the Acoustical Society of America*, 119(5):2618–2627, May 2006.

[7] R. Maier, J. Zillman, A. Roure, M. Winninger, L. Enghardt, U. Tapken, W. Neise, H. Antoine, and E. Bouty. Active control of fan tone noise from aircraft engines. In *7th AIAA/CEAS Aeroacoustics Conference*, Maastricht, Netherlands, 2001.

[8] E Friot, H Bailliet, R Boucheron, J-P Dalmont, R Guillermin, P Herzog, J Laumonier, P-O Mattei, S Meunier, G Poignand, G Rabau, A Roure, J Tartarin, J-C Valière, and M Winninger. Modélisation, contrôle actif et évaluation psycho-acoustique du bruit de soufflante. Rapport final, Réseau Recherche Aéronautique sur le Supersonique, 2003.

[9] S. Elliott. *Signal Processing for Active Control*. Academic Press, London, 2001.

[10] P.A. Nelson and S.J. Elliott. *Active control of sound*. Academic Press, London, 1992.

[11] P. C. Hansen. *Rank-Deficient and Discrete Ill-Posed Problems. Numerical Aspects of Linear Inversion*. SIAM, Philadelphia, 1998.

[12] Julius O. Smith. *Mathematics of the Discrete Fourier Transform (DFT)*. http://-ccrma.stanford.edu/∼jos/mdft/, accessed 2008/01. online book.

[13] M. R. Bai and S. J. Elliott. Preconditioning multichannel adaptive filtering algorithms using evd-and svd-based signal prewhitening and system decoupling. *Journal of Sound and Vibration*, 270(4-5):639–655, March 2004.